Journal of Inorganic Biochemistry 194 (2019) 1–6

Contents lists available at ScienceDirect

Journal of Inorganic Biochemistry

journal homepage: www.elsevier.com/locate/jinorgbio

Anticancer properties of a new non-oxido vanadium(IV) complex with a catechol-modified 3,3′-diindolylmethane ligand

Katja Dankhoff[a], Aamir Ahmad[b], Birgit Weber[a], Bernhard Biersack[c,*], Rainer Schobert[c]

[a] Inorganic Chemistry IV, University of Bayreuth, Universitaetsstrasse 30, 95447 Bayreuth, Germany
[b] USA Mitchell Cancer Institute, 1660 Springhill Avenue, Mobile, AL 36604-1405, USA
[c] Organic Chemistry Laboratory, University of Bayreuth, Universitaetsstrasse 30, 95447 Bayreuth, Germany

ARTICLE INFO

Keywords:
Vanadium
Diindolylmethane
Anticancer drugs
Reactive oxygen species
DNA binding

ABSTRACT

In order to identify new active drug candidates against cancer diseases we investigated the tumor cell growth inhibition, formation of reactive oxygen species, mitochondrial membrane damage, cell cycle arrest and DNA binding activity of a new bis(triethylammonium) tris[1,1-bis(indol-3-yl)-1-(3,4-catecholate)methane]vanadate (IV) complex. It exhibited significant antiproliferative activity against various cancer cell lines, showed a stronger DNA binding than cisplatin and led to mitochondrial damage, a formation of reactive oxygen species, and a cell cycle arrest in the G2/M phase of cancer cells.

1. Introduction

The application of metal-based drugs for the treatment of various diseases has a long history. In terms of metal-based anti-cancer drugs, there are several examples of metallodrugs, which are successfully employed against various tumors [1–4]. Research efforts have mainly focused on the investigation of gold, platinum and ruthenium based anticancer drug candidates [5–7]. But vanadium has also attracted increasing attention for the therapy of tumor diseases and the efforts to investigate vanadium species against cancer have increased over the recent years [8–12]. The formation of reactive oxygen species (ROS) and the interaction with DNA appear to represent the main modes of action of anticancer active vanadium compounds [8,12–14]. The coordination of natural product ligands to vanadium centers is especially intriguing and natural amino acids, for instance, were investigated as suitable ligands for vanadium centers [15–17].

3,3′-Diindolylmethane (DIM), which is a condensation product of the natural product indole-3-carbinol (found in various *Brassica* plants) formed in the stomach upon consumption, displayed significant anticancer activity [18]. In addition, several DIM derivatives with promising anticancer activities were disclosed, in particular, metal-based derivatives such as ferrocene conjugates of DIM [19–23]. Herein, we report on a new homoleptic triscatecholate vanadium(IV) complex **3** bearing di(indol-3-yl)-(3,4-dihydroxyphenyl)methyl ligands (**2**). The ligand **2** itself, which has previously been shown to inhibit HIV-1 integrase [25], was recently tested against cells of HT-29 colon carcinoma, MCF-7 breast cancer and HeLa cervical carcinoma yet displayed no cytotoxic activity after 24 h [24]. We now studied the effects of the coordination of ligand **2** to a vanadium(IV) center on its anti-cancer activity and the possible modes of action of the resulting vanadium(IV)-DIM complex **3**.

2. Experimental

2.1. General

Starting compounds were purchased from Sigma-Aldrich and used without further purification. Compound **2** was prepared according to a literature procedure [26]. Melting points were determined with a Gallenkamp apparatus and are uncorrected. IR spectra were obtained from a Perkin-Elmer One FT-IR spectrophotometer. ^{1}H magnetic resonance (NMR) spectra were recorded under conditions as indicated on a Bruker Avance 300 spectrometer. Chemical shifts (δ) are given in parts per million downfield from TMS as internal standard. ESI (electrospray ionization) mode mass spectra were recorded with a Q-TOF Premier mass spectrometer (Waters, Milford, MA) by direct infusion (10 μL/min). Elemental analyses were carried out with a Perkin-Elmer 2400 CHN elemental analyzer and satisfactory microanalyses (C, ± 0.2, H, ± 0.1) were obtained for the new complex **3**. Redox potentials (cyclic voltammetry) were obtained using a CH Instruments Electrochemical Analyzer (610E) in 0.1 M NBu_4PF_6/MeCN with a platinum electrode, referenced to 0.01 M $AgNO_3$ at room temperature with a scan rate of 50 mV/s. Absorbance spectra were recorded with an Agilent UV/

* Corresponding author.
E-mail address: bernhard.biersack@yahoo.com (B. Biersack).

https://doi.org/10.1016/j.jinorgbio.2019.02.005
Received 14 January 2019; Received in revised form 5 February 2019; Accepted 8 February 2019
Available online 13 February 2019
0162-0134/

Vis spectrophotometer 8453 (Agilent Technologies, USA) in DMF in a spectral range of 300–800 nm at 298 K in quartz cells with 1 cm light-path (Hellma, Germany).

2.2. Chemistry

2.2.1. Bis-(triethylammonium)-tri[1,1-bis-(indol-3-yl)-1-(3,4-catecholate) methane] vanadate(IV) 3

Compound **2** (100 mg, 0.28 mmol) was dissolved in MeOH (5 mL). Vanadyl acetylacetonate (25 mg, 0.093 mmol) was added giving a blue-violet solution. After addition of Et_3N (57 μL, 0.41 mmol) and stirring at room temperature for 5 min the color became more intense and a dark blue-violet precipitate appeared. The formed precipitate was collected, washed with a small amount of cold MeOH and dried in vacuum. Yield: 40 mg (0.031 mmol, 30%); dark-blue solid of mp > 300 °C; ν_{max} (ATR)/cm^{-1} 3403, 3051, 2980, 1571, 1483, 1455, 1417, 1338, 1261, 1246, 1212, 1116, 1094, 1036, 1010, 953, 835, 780, 741; ^{1}H NMR (300 MHz, CD_3OD) δ 1.28 (18H, t, J = 7.4 Hz), 3.07 (12H, d, J = 7.4 Hz), 4.92 (3H, s), 6.8–7.6 (39H, m); m/z (UPLC-Q-TOF, %) 1110.3048 (7), 1109.3341 (23), 1108.3024 (55), 1107.3076 (70), 1106.3015 (12), 1105.2832 (4); Anal. calcd. for $C_{81}H_{80}N_8O_6V$: C, 74.12; H, 6.14. Found: C, 73.92; H, 6.06.

2.3. Cell culture and conditions

518A2 melanoma, HT-29 (ACC-299), HCT-116 (ACC-581), and DLD-1 (ACC-278) colon carcinoma, KB-V1^{Vbl} (ACC-149) cervix carcinoma and MCF-7^{Topo} (ACC-115) breast cancer cells were cultured in Dulbecco's modified Eagle Medium (DMEM, Biochrom) containing 10% fetal bovine serum (FBS; Biochrom) and 1% antibiotic-antimycotic (Thermo Scientific) 37 °C, 5% CO_2, and 95% humidified atmosphere. MCF-7^{Topo} and KB-V1^{Vbl} cells were treated with the maximum-tolerated dose of topotecan and vinblastine, respectively 24 h after every cell passage to keep them multi-drug resistant. Only mycoplasma-free cultures were used.

2.4. MTT assay

Human cancer cells (5 × 10^4 cells/mL, 100 μL/well) were grown in 96-well plates for 24 h and then exposed to various concentrations of **2**, **3** (from freshly prepared stock solutions in DMF), and vehicle (DMF) for 72 h at 37 °C. Then, 12.5 μL of a 0.5% MTT [3-(4,5-dimethylthiazol-2-yl)-2,5-diphenyltetrazolium bromide] solution in PBS was added to reach a final concentration of 0.05% MTT in the wells. After incubating the cells for 2 h, the plates were centrifuged (300 ×g, 5 min, 4 °C) and the supernatant was poured away. The formazan precipitate was solved in DMSO supplemented with 10% SDS and 0.6% acetic acid and incubated for at least 1 h. Then, the absorbance of formazan (λ = 570 nm) and background (λ = 630 nm) were determined with a microplate reader (Tecan). The IC_{50} values were derived from dose inhibition curves as the mean ± standard deviation of four independent assay with respect to control cells set to 100% viability.

2.5. DCFH-DA assay

Reactive oxygen species induced by treatment with the test compounds were determined by the DCFH-DA (2′,7′-dichlorohydrofluorescein diacetate, Sigma Aldrich) assay. Briefly, 518A2 melanoma cells (1 × 10^5 cells/mL, 100 μL/well) were grown for 24 h in black 96-well plates. Then, the cell medium was exchanged for 100 μL of serum-free DMEM supplemented with 20 μM DCFH-DA and the cells incubated for 0.5 h. After washing the cells twice with 100 μL PBS, 100 μL serum-free DMEM was added followed by the treatment with vehicle (DMF), **2** or **3** (5, 10, and 50 μM, from freshly prepared stock solutions) for 1 h. Then, the cells were washed twice with 100 μL PBS. The DCF-fluorescence was measured in 100 μL PBS with a plate reader (Tecan) at λ_{ex} = 485 nm and λ_{em} = 535 nm. The fluorescence of DMF-treated cells was set to 100%. Values exceeding 100% indicate increased ROS concentrations in the cells. The relative ROS production (%) was calculated as the mean ± SD of six independent experiments.

2.6. JC-10 assay

Test compounds' influence on the mitochondrial membrane potential was determined by JC-10 assays (AAT Bioquest). Briefly, 518A2 melanoma cells (1 × 10^5 cells/mL, 100 μL/well) were seeded in black 96-well plates and allowed to adhere for 24 h. Then, the cells were incubated with **2** or **3** (0, 2.5, 5, and 10 μM, from freshly prepared stock solutions) for 24 h. 50 μL JC-10 (60 μM in PBS containing 0.06% pluronic F127) was added to the wells and incubated for 30 min. After washing the cells twice with 100 μL PBS the fluorescence of JC-10 monomeric form at λ_{ex} = 490 nm, λ_{em} = 535 nm and that of JC-10 aggregates at λ_{ex} = 490 nm, λ_{em} = 590 nm was measured with a microplate reader (TECAN) in 100 μL PBS. The ratio of aggregates to monomeric form as a measure of the degree of mitochondrial damage was determined in quadruplicate with the vehicle treated control cells set as 100%.

2.7. Cell cycle analysis

518A2 melanoma cells (5 × 10^4 cells/mL, 3 mL/well) were grown for 24 h in 6 wells plates and then treated with vehicle (DMF), **2** (20 μM), and **3** (3 μM, from freshly prepared stock solutions) for 24 h at 37 °C. The cells were harvested by trypsination and fixed in 1 mL 70% EtOH for at least 24 h. After centrifugation (400 ×g, 5 min), the supernatant was withdrawn and the cells pellet washed with 1 mL PBS. Then, the cells were treated with PI staining solution (50 μg/mL propidium iodide; 0.1% sodium citrate, 50 μg/mL RNase A in PBS) for 30 min for digesting RNA and staining DNA. The fluorescence intensity of 10,000 single cells was measured at λ_{em} = 570 nm (λ_{ex} = 488 nm laser source) with a Beckmann Coulter Cytomics FC 500 flow cytometer. The percentages of cells in the different phases of the cell cycle (G1, S and G2/M phase) were determined using the CXP Analysis software (Beckmann Coulter). The percentage of apoptotic cells was derived from sub-G1 peaks.

2.8. Ethidium bromide assay

Salmon sperm DNA (10 μg/mL in TE buffer; 100 μL/well; Sigma Aldrich) was pipetted in black 96-well plates and treated with vehicle, compounds **2** or **3** (from freshly prepared stock solutions), and cisplatin (25, 50, and 100 μM) for 2 h at 37 °C. Then, ethidium bromide (10 μg/mL in TE buffer, 100 μL/well) was added and after 5 min of incubation the fluorescence (λ_{ex} = 535 nm, λ_{em} = 595 nm) was measured for each well with a microplate reader (Tecan). Each value was corrected by ethidium bromide background (samples without DNA). The resulting values were calculated as percent of vehicle (100% fluorescence = 100% ethidium bromide binding). Reduced fluorescence indicates impaired ethidium bromide-DNA adducts due to intercalation sites being blocked by the test compounds. The values are the means ± SD of experiments carried out in triplicate.

3. Results and discussion

3.1. Chemistry

The catechol modified DIM-based ligand **2** was prepared by reaction of 3,4-dihydroxybenzaldehyde with two equivalents of indole [26]. Complex **3** was obtained as a dark-blue solid from the reaction of three equivalents of **2** with oxidovanadium acetylacetonate **1** after treatment with Et_3N (Scheme 1) [27].

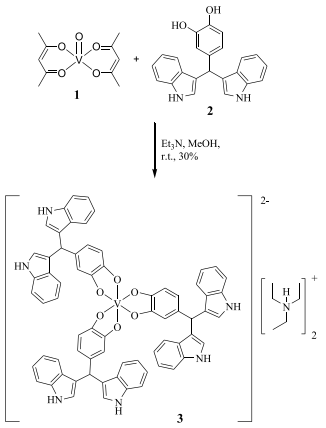

Scheme 1. Synthesis of complex **3**.

Table 1
Inhibitory concentrations (IC_{50}, μM)[1] of **2** and **3** when applied to human 518A2 melanoma, HT-29, HCT-116^{wt} and HCT-116^{-p53} colon carcinoma, KB-V1^{Vbl} cervix carcinoma, MCF-7^{Topo} and MDA-MB-231 mamma carcinoma, and Panc-1 and BxPC-3 pancreatic carcinoma cells. Tumor selectivity index (SI), IC_{50} > 40 μM (MCF-10A)/IC_{50} (cancer cells) of compound **3**.

	2	3	SI
518A2	16.9 ± 2.0	3.0 ± 0.4	> 13.3
HT-29	48.9 ± 1.4	8.5 ± 0.4	> 4.7
HCT-116^{wt}	7.2 ± 0.6	1.8 ± 0.1	> 22
HCT-116^{-p53}	7.8 ± 0.4	2.1 ± 0.1	> 19.0
KB-V1^{Vbl}	43.7 ± 3.0	6.8 ± 0.2	> 5.9
MCF-7^{Topo}	25.7 ± 6.7	14.7 ± 1.6	> 2.7
MDA-MB-231	19.7 ± 2.0	2.5 ± 0.1	> 16
Panc-1	9.5 ± 0.1	1.8 ± 0.1	> 22.2
BxPC-3	24.1 ± 2.1	2.5 ± 0.1	> 16

[1]Values are derived from dose-response curves obtained by determining the percentage of viable cells relative to vehicle treated controls after 72 h treatment with the test compounds using MTT-assays; values are the means ± SD of four independent experiments.

3.2. Antiproliferative activity

The antiproliferative activities of **2** and **3** were tested (by MTT assays) against seven cancer cell lines of five entities (Table 1) [28]. In addition, compound **3** was tested against non-malignant human MCF-10a breast epithelial cells (Fig. 1). Both compounds showed dose dependent inhibition curves against all tested cancer cell lines with IC_{50} values ranging from low single-digit to double-digit micromolar concentrations. The ligand **2** was on average five times less active than the corresponding vanadium complex **3**. HT-29 colon carcinoma and the multidrug resistant KB-V1^{Vbl} cervix carcinoma cells, which overexpress ABC transporters of the P-gp type, were least sensitive towards the treatment with the test compounds whereas the test compounds were most active against HCT-116^{wt} (wildtype) colon carcinoma and Panc-1 pancreatic carcinoma cells. The growth inhibitory activities of **2** and **3** were independent of p53 function as to results obtained from the HCT-116^{-p53} cells. In addition, the viability of non-malignant MCF-10A breast epithelial cells treated with 40 μM of **3** was about 80% when compared to vehicle treated control cells. Thus, **3** showed a distinct tumor selectivity which was expressed by the tumor selectivity index (SI, Table 1). It depicts the ratio of the IC_{50} value against the non-malignant MCF-10A breast epithelial cells (IC_{50} > 40 μM) and the tested cancer cell lines. The greater the SI, the more selective the test compound **3**. For Panc-1 pancreatic carcinoma and HCT-116 colon carcinoma cells excellent SI values greater 20 were calculated for **3**. For 518A2 melanoma cells the SI value exceeded 10 whereas it was only about 5 for HT-29 colon carcinoma and KB-V1^{Vbl} cervix carcinoma cells.

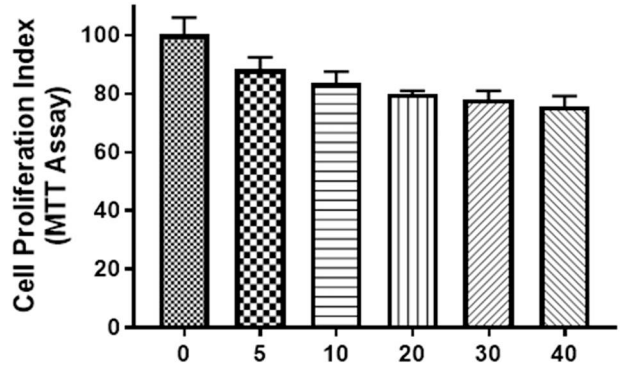

Fig. 1. Growth inhibition of compound **3** after 72 h when applied to human MCF-10A breast epithelial cells (MTT assay). Experiments were repeated at least three times with quadruplet observations in every repeat.

We observed that the growth inhibitory activity of samples of complex **3** in DMF stock solutions was distinctly reduced as early as 24 h after the preparation of the stock solution. Therefore, the stability of complex **3** in DMF solution was investigated by UV/Vis spectrophotometry over a period of 72 h (Fig. 2). We found that the UV/Vis spectra of freshly prepared solutions and of solutions standing for 24 h, 48 h, and 72 h differed significantly. Thus, we applied freshly prepared stock solutions of complex **3** for all of the following bioassays.

3.3. Electrochemical properties and ROS formation

The redox properties of complex **3** were investigated via cyclic voltammetry. Interestingly, the cyclic voltammogram of **3** in acetonitrile showed a distinct, irreversible reduction of the complex anion at −0.59 V vs. Ag/$AgNO_3$ (Fig. 3B). It appeared tidier and more waveless than the cyclic voltammogram of ligand **2**, indicative of a stabilization of the latter against redox reactions by coordination to the vanadium center (Fig. 3A, B). Spontaneous reductions of neutral oxido and non-oxidovanadium(IV) complexes to vanadium(III) complexes upon addition of 2,2′-bipyridine and 1,8-hydroxyquinoline chelate ligands had been reported before [29,30]. In these cases the intermediate cationic vanadium(IV) chelate species were reduced reversibly at more positive potentials than that of the standard Fc/Fc^+ in cyclic voltammetry experiments.

The formation of reactive oxygen species such as superoxides and peroxides is one of the main consequences of the treatment of cells with vanadium complexes. The effects of the ligand **2** and complex **3** on the

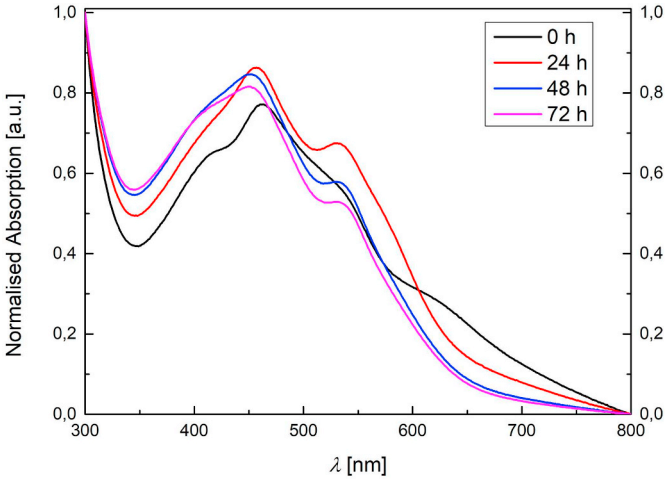

Fig. 2. UV/Vis spectra of complex **3** (0.047 mg/mL, DMF, 298 K) at the indicated time points.

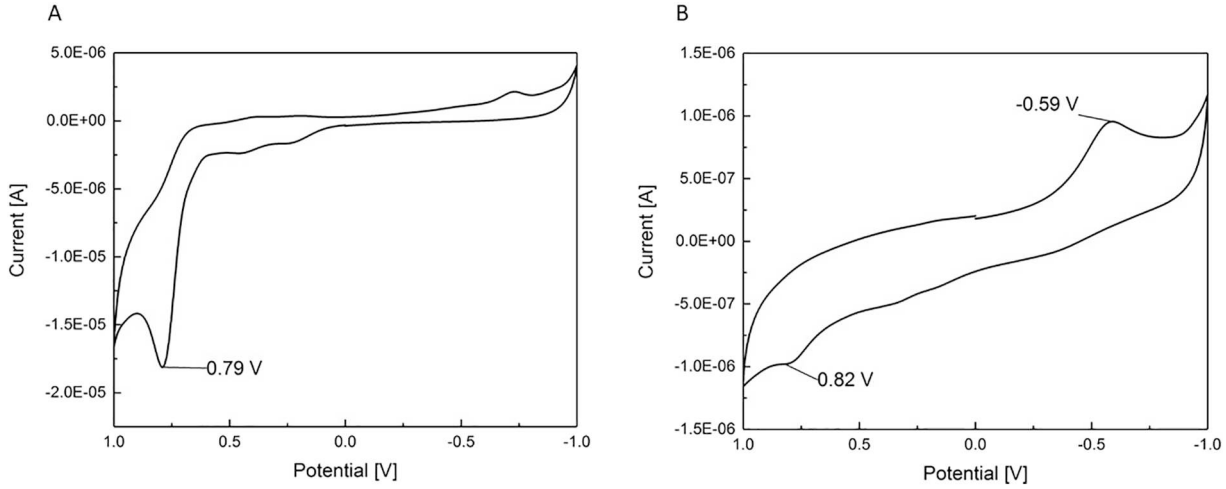

Fig. 3. Cyclic voltammogram (acetonitrile, 0.1 M NBu_4PF_6, 50 mV/s, vs. $Ag/AgNO_3$) of ligand **2** (A) and vanadium(IV) complex **3** (B).

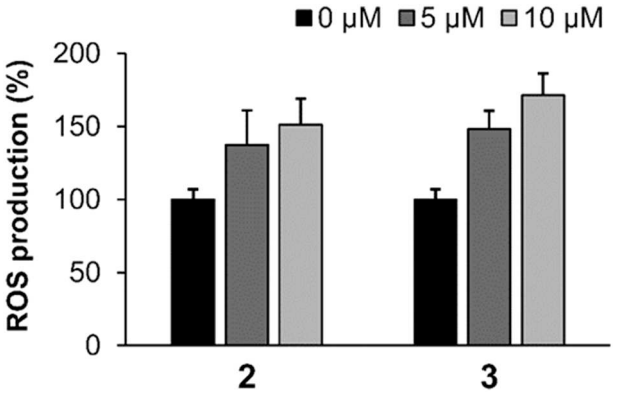

Fig. 4. Concentrations of ROS in 518A2 melanoma cells treated with compounds **2** or **3**. Cells were pretreated with DCFH-DA (20 µM, 30 min) and then incubated with the test compounds **2** and **3** (0, 5, and 10 µM; 1 h). The intensity of the green DCF fluorescence as a measure of the intracellular ROS level was set to 100% for vehicle (DMF) treated control cells. The ROS production (%) was depicted as the mean ± SD of five independent experiments.

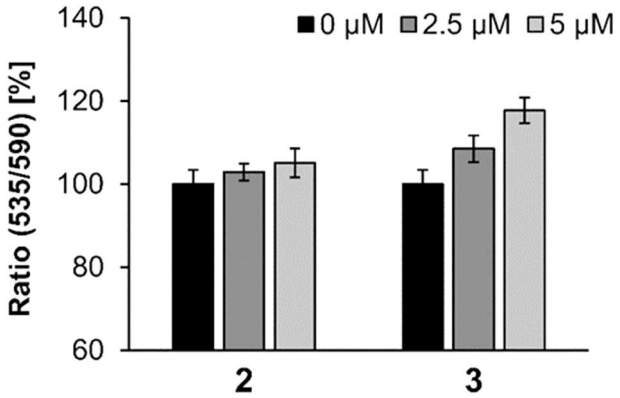

Fig. 5. Effects on the mitochondrial membrane potential of 518A2 cells as observed in JC-10 assays with cells treated with **2** or **3** (0, 2.5, 5, and 10 µM; 24 h). Increasing ratios of fluorescence at 535 nm (JC-10 mono adduct) to that at 590 nm (JC-10 aggregate) indicate the decrease of the mitochondrial membrane potential. Values are the means ± SD of four independent experiments.

ROS level in 518A2 melanoma cells were determined by a DCFH-DA (2′,7′-dichlorohydrofluorescein diacetate) assay which is based on the deacetylation of DCFH-DA to DCFH (2′,7′-dichlorohydrofluorescein) by esterases and the following oxidation to the fluorescent DCF (2′,7′-dichlorofluorescein). Ligand **2** and even slightly more so its vanadium complex **3** led to increased levels of unspecified ROS in 518A2 melanoma cells of up to > 150% relative to untreated controls (Fig. 4).

3.4. Mitochondrial damage

Various vanadium compounds are known to disrupt the mitochondrial membrane potential [31]. Thus, the effect of vanadium(IV) complex **3** on the mitochondrial membrane potential of 518A2 melanoma cells was evaluated by the JC-10 assay and compared with the effect of its free catechol ligand **2** (Fig. 5). Complex **3** initiated a concentration dependent reduction of the number of cells with intact mitochondria indicated by increasing ratios of fluorescence at 535 nm (JC-10 mono adduct) to that at 590 nm (JC-10 aggregate). Upon treatment of the cells with complex **3** this ratio was increased to 120% when compared with untreated control cells. In contrast to **3**, the ligand **2** left the ratio virtually unaltered.

3.5. Effects on the cell cycle progression

The effect of the test compounds **2** and **3** on the cell cycle progression in 518A2 melanoma cells was measured by flow cytometry after staining the DNA with propidium iodide (PI). It is known that DIM induces $p27^{Kip}$ in various cancer cells, which indicates the arrest of cells in G1 phase of the cell cycle [32]. Indeed, treatment of 518A2 melanoma cells with 25 µM of **2** reduced the percentage of cells in S-phase whereas the number of cells in G1 and G2/M phases was distinctly increased. In contrast, complex **3** arrested the cells in G2/M phase (Fig. 6). In addition, both compounds **2** and **3** caused only a negligible change in the proportion of apoptotic cells in sub-G1. A G2/M arrest of melanoma cells has been reported for another anti-melanoma active vanadium complex recently [33]. It should be noted that cisplatin and a *cis*-dichlorido[(1,3-dibenzyl)imidazole-2-ylidene](dimethyl sulfoxide) platinum(II) complex also initiated an accumulation of 518A2 melanoma cells in the G2/M phase [34].

3.6. DNA interaction

DNA represents one of the main targets of certain vanadium complexes [35–38]. Therefore, the interaction of vanadium complex **3** with DNA was tested by the ethidium bromide assay and compared with the DNA-binding activity of ligand **2**. The gold standard of DNA binders, cisplatin, was used as a positive control. In this assay, salmon sperm DNA

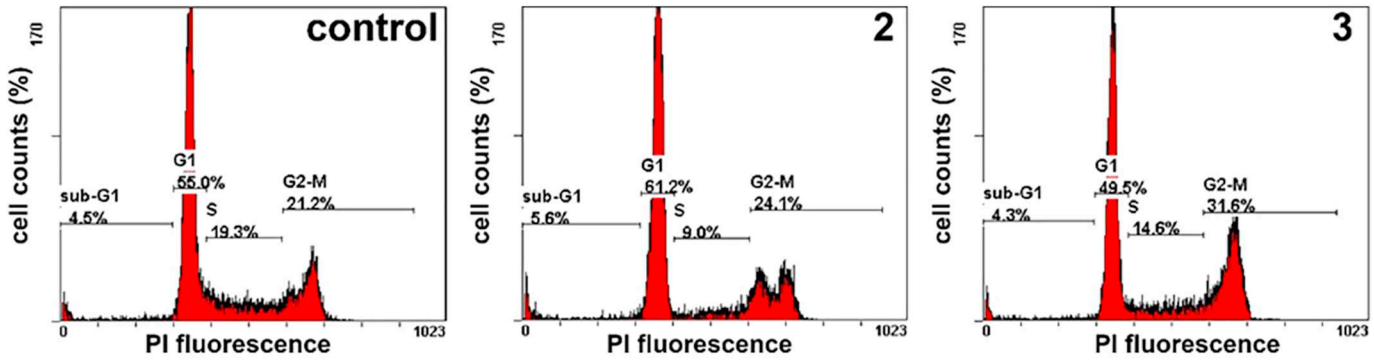

Fig. 6. Effect of **2** and **3** on the cell cycle progression of 518A2 melanoma cells. Cells were treated with **2** (25 μM), **3** (5 μM), or vehicle (DMF) for 24 h. Typical cell cycle profiles and percentage of cells in G1, S, and G2-M phase as well as the proportion of sub-G1 events (apoptotic cells) as determined by flow cytometry after DNA staining with propidium iodide (PI) of three independent experiments.

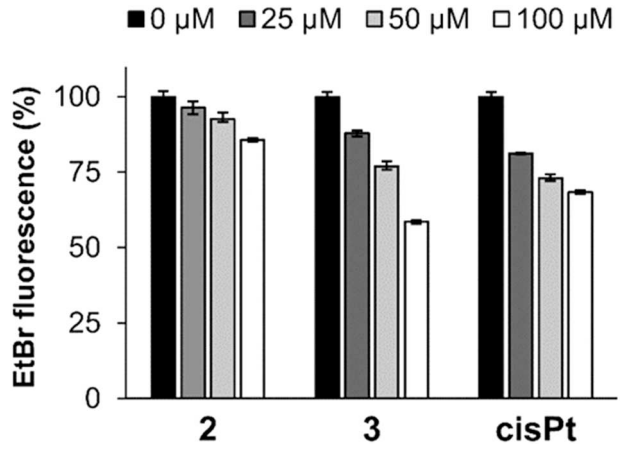

Fig. 7. Relative ethidium bromide-DNA adduct fluorescence after pre-incubation with vehicle (DMF; set to 100%), cisplatin, **2**, and **3** (25, 50, and 100 μM; 2 h). Decreased ethidium bromide fluorescence signifies the inhibition of ethidium bromide intercalation into DNA already modified by the test compounds.

was first incubated with the test compounds for 2 h followed by incubation with ethidium bromide (EtBr) for 30 min. Reduced intensities of EtBr fluorescence indicate the prevention of EtBr intercalation into the DNA due to the already established interaction of the test compounds with the latter. Hence, the degree of EtBr fluorescence decrease is a measure of the degree of DNA interaction of the test compounds. Pre-incubation of DNA with **2** caused a slight decrease of EtBr fluorescence to 85% at the highest concentration of the test compound. The interaction of **3** with DNA was distinctly more pronounced and exceeded the reduction of EtBr fluorescence caused by cisplatin. At the highest concentration, complex **3** reduced the EtBr fluorescence of DNA to 59% compared with that of vehicle treated DNA whereas cisplatin only decreased it to 68% (Fig. 7). The exact mode of DNA interaction by vanadium complex **3** is not yet known and may include coordination processes as well as DNA-strand breaks via formed ROS.

4. Conclusions

The new vanadate(IV) complex **3** bearing three catechol-modified DIM ligands displayed distinct anticancer activity in our studies. It inhibited tumor cell growth, led to increased ROS formation and to a decrease of the mitochondrial membrane potential. In addition, complex **3** showed some similarities to cisplatin concerning DNA interaction and cell cycle arrest (G2/M arrest) as signs for a considerable anticancer potential. Since biological studies of catecholato-vanadate complexes are rare, the results now obtained for complex **3** will add significantly to a better understanding of their modes of anticancer action.

Abbreviations

DCFH-DA	2′,7′-dichlorohydrofluorescein diacetate
DIM	3,3′-diindolylmethane
ESI	electrospray ionization
EtBr	ethidium bromide
MTT	3-(4,5-dimethylthiazol-2-yl)-2,5-diphenyltetrazolium bromide
PI	propidium iodide
ROS	reactive oxygen species

Acknowledgments

R.S. thanks the Deutsche Forschungsgemeinschaft for financial support (grant Scho 402/12-1). We thank Dr. Florian Schmitt (University of Bayreuth) for technical assistance and Dr. Holger Schmidt (University of Bayreuth) for high resolution mass spectra.

References

[1] P. Martins, M. Marques, L. Coito, A.J. Pombeiro, P.V. Baptista, A.R. Fernandes, Anticancer agents, Med. Chem. 14 (2014) 1199–1212.
[2] G. Gasser, N. Metzler-Nolte, Curr. Opin. Chem. Biol. 16 (2012) 84–91.
[3] C.G. Hartinger, N. Metzler-Nolte, P.J. Dyson, Organometallics 31 (2012) 5677–5685.
[4] I. Ott, R. Gust, Arch. Pharm. 340 (2007) 117–126.
[5] S. Nobili, E. Mini, I. Landini, C. Gabbiani, A. Casini, L. Messori, Med. Res. Rev. 30 (2010) 550–580.
[6] B. Biersack, Mini-Rev. Med. Chem. 16 (2016) 804–814.
[7] T.C. Johnstone, K. Suntharalingam, S.J. Lippard, Chem. Rev. 116 (2016) 3436–3486.
[8] J.C. Pessoa, J. Inorg. Biochem. 147 (2015) 4–24.
[9] A.M. Evangelou, Crit. Rev. Oncol. Hematol. 42 (2002) 249–265.
[10] L. Novotny, S.B. Kombian, J. Cancer. Res. Updat. 3 (2014) 97–102.
[11] K.H. Thompson, C. Orvig, Coord. Chem. Rev. 219 (2001) 1033–1053.
[12] E. Kioseoglou, S. Petanidis, C. Gabriel, A. Salifoglou, Coord. Chem. Rev. 301-302 (2015) 87–105.
[13] J.C. Pessoa, E. Garriba, M.F.A. Santos, T. Santos-Silva, Coord. Chem. Rev. 301-302 (2015) 49–86.
[14] J. Benitez, L. Guggeri, I. Tomaz, J.C. Pessoa, V. Moreno, J. Lorenzo, F.X. Aviles, B. Garat, D. Gambino, J. Inorg. Biochem. 103 (2009) 1386–1394.
[15] J.C. Pessoa, I. Cavaco, I. Correia, D. Costa, R.T. Henriques, R.D. Gillard, Inorg. Chim. Acta 305 (2000) 7–13.
[16] I. Cavaco, J.C. Pessoa, S.M. Luz, M.T. Duarte, P.M. Matias, R.T. Henriques, R.D. Gillard, Polyhedron 14 (1995) 429–439.
[17] C. Gabriel, M. Kaliva, I. Venetis, P. Baran, I. Rodriguez-Escudero, G. Voyiatzis, M. Zervou, A. Salifoglou, Inorg. Chem. 48 (2009) 476–487.
[18] F.H. Sarkar, Y. Li, Cancer Treat. Rev. 35 (2009) 597–607.
[19] P. Lei, M. Abdelrahim, S.D. Cho, X. Liu, S. Safe, Mol. Cancer Ther. 7 (2008) 3363–3372.
[20] C. Qin, D. Morrow, J. Stewart, K. Spencer, W. Porter, R. Smith III, T. Phillips, M. Abdelrahim, I. Samudio, S. Safe, Mol. Cancer Ther. 3 (2004) 247–260.
[21] S. Chintharlappalli, R. Burghardt, S. Papineni, S. Ramaiah, K. Yoon, S. Safe, J. Biol. Chem. 280 (2005) 24903–24914.
[22] R. Contractor, I.J. Samudio, Z. Estrov, D. Harris, J.A. McCubrey, S.H. Safe, M. Andreeff, M. Konopleva, Cancer Res. 65 (2005) 2890–2898.
[23] J.K. Muenzner, A. Ahmad, M. Rothemund, S. Schrüfer, S. Padhye, F.H. Sarkar,

R. Schobert, B. Biersack, Appl. Organometal. Chem. 30 (2016) 441–445.
[24] K. Naidu, S.I. Khalivulla, S. Rasheed, S. Fakurazi, P. Arulselvan, O. Lasekan, F. Abas, Int. J. Mol. Sci. 14 (2013) 1843–1853.
[25] J. Deng, T. Sanchez, N. Neamati, J.M. Briggs, J. Med. Chem. 49 (2006) 1684–1692.
[26] D. Maciejewska, M. Rasztawicka, I. Wolska, E. Anuszewska, B. Gruber, Eur. J. Med. Chem. 44 (2009) 4136–4147.
[27] S.R. Cooper, Y.B. Koh, K.N. Raymond, J. Am. Chem. Soc. 104 (1982) 5092–5102.
[28] T. Mosmann, J. Immunol. Methods 65 (1983) 55–63.
[29] M.J. Manos, A.J. Tasiopoulos, C. Raptopoulou, A. Terzis, J.D. Woollins, A.M.Z. Slawin, A.D. Keramidas, T.A. Kabanos, J. Chem. Soc. Dalton Trans. (2001) 1556–1558.
[30] M. Rikkou, M. Manos, E. Tolis, M.P. Sigalas, T.A. Kabanos, A.D. Keramidas, Inorg. Chem. 42 (2003) 4640–4649.
[31] Y. Zhao, L. Ye, H. Liu, Q. Xia, Y. Zhang, X. Yang, K. Wang, J. Inorg. Biochem. 104 (2010) 371–378.
[32] Z. Wang, W.Y. Bennett, K.W. Rahman, F. Ahmad, F.H. Sarkar, Mol. Cancer Ther. 7 (2008) 341–349.
[33] C. Rozzo, D. Sanna, E. Garribbia, M. Serra, A. Cantara, G. Palmieri, M. Pisano, J. Inorg. Biochem. 174 (2017) 14–24.
[34] J.K. Muenzner, T. Rehm, B. Biersack, A. Casini, I.A.M. de Graaf, P. Worawutputtapong, A. Noor, R. Kempe, V. Brabec, J. Kasparkova, R. Schobert, J. Med. Chem. 58 (2015) 6283–6292.
[35] P. Köpf-Maier, H. Köpf, Chem. Rev. 87 (1987) 1137–1152.
[36] H. Du, J. Xiang, Y. Zhang, Y. Tang, G. Xu, J. Inorg. Biochem. 102 (2008) 146–149.
[37] H. Sakurai, H. Tamura, K. Okatani, Biochem. Biophys. Res. Commun. 206 (1995) 133–137.
[38] N. Butenko, A.I. Tomaz, O. Nouri, E. Escribano, V. Moreno, S. Gama, V. Ribeiro, J.P. Telo, J.C. Pessoa, I. Cavaco, J. Inorg. Biochem. 103 (2009) 622–632.